

See discussions, stats, and author profiles for this publication at: <https://www.researchgate.net/publication/283620315>

Targeting Wnt Canonical Signaling by Recombinant sFRP1 Bound Luminescent Au-Nanocluster Embedded Nanoparticles in Cancer Thernostics

ARTICLE · NOVEMBER 2015

DOI: 10.1021/acsbiomaterials.5b00305

READS

74

5 AUTHORS, INCLUDING:



Upashi Goswami

Indian Institute of Technology Guwahati

6 PUBLICATIONS 8 CITATIONS

[SEE PROFILE](#)



Amaresh Kumar Sahoo

Indian Institute of Technology Guwahati

16 PUBLICATIONS 55 CITATIONS

[SEE PROFILE](#)

Targeting Wnt Canonical Signaling by Recombinant sFRP1 Bound Luminescent Au-Nanocluster Embedded Nanoparticles in Cancer Theranostics

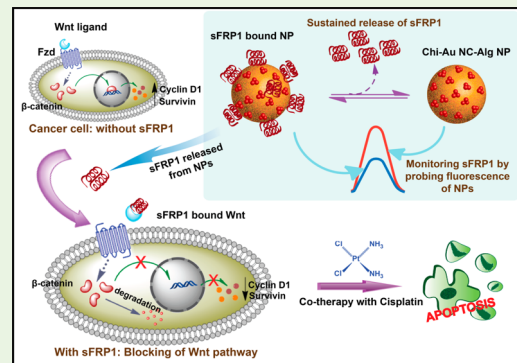
Archita Ghoshal,[†] Upashi Goswami,[‡] Amresh Kumar Sahoo,[‡] Arun Chattopadhyay,^{§,‡} and Siddhartha Sankar Ghosh^{*,†,‡}

[†]Department of Biosciences and Bioengineering, [‡]Centre for Nanotechnology and [§]Department of Chemistry, Indian Institute of Technology Guwahati, Guwahati-781039, Assam, India

 Supporting Information

ABSTRACT: Secreted frizzled-related protein 1 (sFRP1) is a natural blocker of the Wnt signaling pathway in normal adult cells but is epigenetically silenced in cancer cells leading to aberrant proliferation. In this study, we have reported novel composite nanoparticles fabricated with gold nanocluster embedded chitosan and alginate, bound to bacterially expressed human recombinant sFRP1. The Wnt pathway, which is upregulated in cancer, has been specifically targeted with the nanoparticles to achieve an antiproliferative effect on cancer cells, as evident from reduced levels of downstream molecules, namely, β -catenin, cyclin D1, and survivin. The nanoparticles enabled sustained release of sFRP1 outside the cells, where it is functional. Moreover, remarkable luminescence properties of gold nanoclusters were exploited for binding, imaging, and tracking studies. Co-therapy of sFRP1-loaded nanoparticles with the drug cisplatin targeted two independent pathways to induce apoptosis, as documented by flow cytometry based assays. Overall, this nanosystem is promising for tracking, imaging, and targeting cancer signaling with therapeutic protein.

KEYWORDS: nanoparticle, gold nanocluster, secreted frizzled-related protein 1 (sFRP1), Wnt signaling pathway, cancer cotherapy



INTRODUCTION

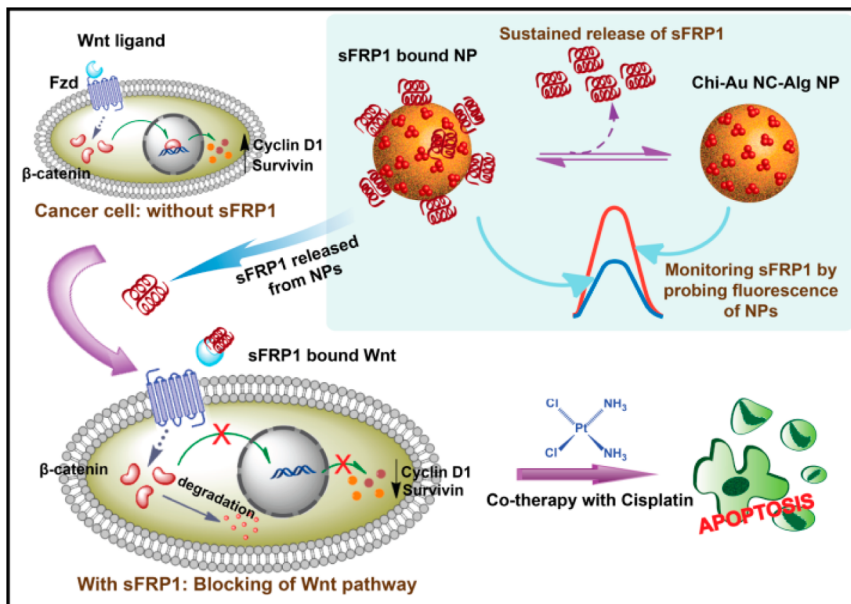
Cell signaling molecule loaded nanoparticles have attracted tremendous attention in the novel area of theranostics for combating complex diseases like cancer.^{1,2} Cure of cancer has proven to be greatly elusive to molecular biologists and chemists alike. Adverse side effects of conventional chemotherapeutic drugs, like doxorubicin^{3,4} and cisplatin,⁵ along with the development of multidrug resistance have led to the search for alternatives. Immunotherapy based treatment options have been in the process of being perfected for decades.⁶ Interleukin-2 is the first effective adoptive immunotherapy, which involves boosting the patient's immune system by expanding the T-cell population.^{7,8} Another exciting avenue of research has been the more recent approach of recombinant protein therapy to target specific cell signaling pathways in cancer. One such prospective target is the canonical or classical Wnt pathway, shown to be aberrantly upregulated in cancer, culminating in the activation of several pro-proliferative genes.^{9,10} However, this pathway is naturally blocked by a group of cell proliferation regulating glycoproteins, called the secreted frizzled-related proteins (sFRPs), in normal adult cells.^{11–14} Of these, sFRP1, which was the first discovered sFRP, is known to be epigenetically silenced in various cancers, like, colorectal, breast, ovarian, malignant mesothelioma, and lung cancer.^{15–18} Several studies

have demonstrated that transfection of sFRP1, in breast cancer¹⁹ and hepatoma cell lines,²⁰ has effectively inhibited cell growth. However, sFRP1 had never been used in the form of recombinant therapeutic protein before we reported that its administration on cervical and breast cancer cell lines effected significant reduction of cell proliferation and sensitized the cells toward chemotherapy.²¹ However, the addition of a therapeutic protein exogenously may have certain limitations pertaining to the fact that slight changes in its microenvironment during delivery can destabilize the protein, resulting in its loss of function. The constraints, thus arising, can be circumvented by fabricating a system ensemble to stabilize and enhance the efficacy of the protein, for sustained release of payload as well as to probe and quantify the release profile of the protein. However, maintenance of the structural and functional integrity of the macromolecules should be given prime importance for the design of these delivery systems.

Presently, in healthcare, these challenges are being encountered by the advancements in nanomedicine, where nanocarriers are in the process of taking center stage in modern

Received: July 16, 2015

Accepted: November 2, 2015

Scheme 1. Schematic Representation of the Findings of This Study

clinical applications. Biocompatible nanoparticles (NPs), which are stable in aqueous environments, have enhanced half-life values, and disintegrate to nontoxic metabolites, are given preference in clinical usage.²² Fluorescent NPs are evolving as a promising tool for theranostic purposes.^{23,24} In particular, metal nanoclusters (NCs), possessing extraordinary physical and chemical properties, have the potential to revolutionize the current therapeutic modality.^{25–27} Of the metal NCs, gold nanoclusters (Au NCs) have transpired as an attractive option due to their stability, nontoxicity, remarkable fluorescence properties, and large Stokes shift, thus overcoming the limitations of organic dyes and quantum dots.^{28–31} Their emission in the red/near-infrared (NIR) region prevents interference from biological entities during cellular imaging.^{32–34} Biodegradable polymers, acting as templates for hosting Au NCs, may qualify as versatile platforms for drug delivery, as they can be used as a probe for the detection of binding and release of cargo. In addition, tunable fluorescence imaging studies can provide a thorough understanding of its mechanism of action, making it an attractive solution for a grave problem. Our group has previously reported the synthesis of chitosan based Au NC containing nanocarriers, displaying simultaneous red, green, and blue fluorescence, which has been favorably exploited for optical imaging and as a flow cytometry probe.³⁵ Combination therapy has also been implemented using Au NCs for fluorescent/X-ray computed tomography imaging and radiotherapy.^{36,37}

Recent material innovations have propagated a paradigm shift toward the unique concept of the codelivery of drug and therapeutic molecules conjugated to nanocarriers.³⁸ Studies have revealed that these therapeutic molecules by themselves may not be toxic enough to eradicate cancer completely but that they may be used in combination with chemotherapy to help reduce the dosage of drugs and diminish their side effects.^{39,40} Ligand-targeted NPs loaded with chemotherapeutic drugs are increasingly finding application in the remedy of cancer, with the common targets being receptors overexpressed by cancer cells, such as folate and transferrin receptors.^{41–43} However, even though aberrant upregulation of the Wnt

pathway is one of the highlights in cancer, to date there has been no report documenting the targeting of the Wnt pathway with NPs for cancer therapy.

In the current study, we establish a novel system consisting of recombinant therapeutic protein sFRP1 bound chitosan-Au NC-alginate composite NPs (henceforth referred to as protein-NPs) for specific targeting of the Wnt pathway in cervical cancer cells (HeLa). The antiproliferative effect of the sFRP1-NPs was determined by treating HeLa cells. Here, the theranostic NPs were constructed by a quick and facile method, whereby Au NCs were synthesized keeping the biopolymer chitosan as template and converted to NPs using polysaccharide alginate. Size and surface charge of these multifunctional NPs were modulated keeping in mind that recombinant sFRP1 binds to its target Wnt ligand in the extracellular space, and hence, the composite ideally should not penetrate the cell membrane. Luminescence properties of Au NCs fortified their role as a fluorescent signal indicator for *in media* probing of protein and monitoring its binding, stability, and imaging over a prolonged time period. Binding of sFRP1 with NPs resulted in its enhanced antiproliferative activity, as shown by a cell viability assay, dual staining by acridine orange and ethidium bromide, cell cycle analysis, and an apoptosis detection assay of treated HeLa cells. Targeting of Wnt ligands with sFRP1-NPs successfully blocked the Wnt signaling cascade, which plays a predominant role in carcinogenesis. The uniqueness of this regime lies in the feature that the therapeutic protein-NPs will simultaneously serve the purposes of both targeting cancer cells and arresting their growth. In addition, the synergistic effect of sFRP1-NPs with traditional chemotherapeutic agent cisplatin brought about a drastic increase in apoptotic cell population. This novel approach of cotherapy exploited the benefits of NP-mediated protein therapeutics to augment the efficacy of chemotherapy via targeted cancer cell signaling. While sFRP1 possesses the therapeutic potential, composite NPs provide stability to the system. The crux of the concept of this work has been illustrated in Scheme 1.

MATERIALS AND METHODS

Synthesis of Chitosan-Au NC-Alginate NPs (Chi-Au NC-Alg NPs). Chitosan solution was prepared at a concentration of 0.5% in 0.1% (v/v) acetic acid. It was then filtered to attain a homogeneous solution of chitosan. The pH was adjusted to 6.2 with NaOH. Two milliliters of this solution was added to 10 mL of Milli-Q water, to which 80 μ L of 0.11 M MPA was added. Au NC was synthesized by adding 180 μ L of 10 mM gold(III) chloride to the above solution and stirring for 15 min at room temperature. After checking the luminescence of Au NCs in an UV transilluminator, 2 mL of the synthesized chitosan-Au NC was taken in a separate tube. To make negatively charged NPs, 1 mL of liquid paraffin oil was added to it, along with 0.5 mL of 1% sodium alginate. It was then sonicated with a probe sonicator for 3 min, under cold conditions. After sonication, the top layer of oil was discarded, and the rest was centrifuged at 11,500 g for 5 min at room temperature. The pellet obtained on centrifugation was resuspended in 1 mL of Milli-Q water. This washing step was crucial for the complete removal of oil and hence was repeated three times. After the final round of centrifugation, the pellet was dissolved in 500 μ L of Milli-Q water to get negatively charged chitosan-Au NC-alginate NPs.

Expression and Purification of GST Tagged Human sFRP1. Protein was expressed in *E. coli* BL21 (DE3) cells transformed with a recombinant vector pGEX-4T2 containing the human sFRP1 gene. GST-sFRP1 was purified to near homogeneity by affinity chromatography, using glutathione-agarose beads, which bind to GST.²¹ The purified GST tagged human SFRP1 protein was dialyzed against 10 mM tris buffer at pH 7.5 for 7 h. Protein concentration was estimated by the Bradford assay for all experiments.

Characterization of Chi-Au NC-Alg NPs. The NPs were characterized, alone as well as after binding to GST-sFRP1, by means of dynamic light scattering (DLS) and zeta potential measurement using a Malvern Zetasizer Nano ZS, to determine hydrodynamic diameter and net surface charge, respectively. Fourier transform infrared (FTIR) spectroscopic analysis was also performed for NPs, protein, and protein-NPs. Samples were lyophilized, pellets were prepared with potassium bromide, and, thereafter, spectral measurements were taken in the range of 400 to 4000 cm^{-1} using PerkinElmer Spectral One. Quantum yield of Chi-Au NC-Alg NPs was calculated using an established formula⁴⁴ (details are given in Supporting Information).

Imaging of Chi-Au NC-Alg NPs with TEM and a Fluorescence Microscope. Transmission electron microscopy (JEM 2100 TEM) was done, at an accelerating voltage of 200 keV, to capture images of NPs, alone and bound to GST-sFRP1. For this purpose, samples were drop-casted on carbon coated copper grid and dried at room temperature. Fluorescence microscopy was also used to record images of NPs at different emission wavelengths by drying the samples on a glass slide.

Binding Studies of NPs with Protein. The same batch of NPs was loaded with different amounts of dialyzed protein for studying their binding efficiency. The volume was made up to 1 mL with 10 mM tris buffer (pH 7.5) for all samples. Incubation was done at 37 °C for 3 h, at the end of which, samples were centrifuged and the pellet was redispersed in 1 mL of Milli-Q. Luminescence of NPs was probed at an excitation wavelength of 320 nm using Fluorolog-3. The binding efficiency was calculated by the following formula:

$$\text{binding efficiency}(\%) = \frac{\text{intensity}_{\text{NP}} - \text{intensity}_{\text{protein-NP}}}{\text{intensity}_{\text{NP}}} \times 100$$

Circular dichroism spectral analysis was conducted with a JASCO-815 spectrometer (Jasco, Japan), at a flow rate of 5 L/min, a temperature of 25 °C, and scanning wavelengths of 240 to 190 nm.

Release Studies of Protein. From the previous experiment, the concentration of protein displaying maximum binding to the NPs was selected. After binding, samples were centrifuged, pellets were redispersed in phosphate buffered saline (PBS), and incubated at 37 °C for different time periods ranging from 0 to 48 h. Each sample was centrifuged at various time points, and the supernatant was collected,

which will contain the released protein. For this experiment, the fluorescence intensity of the released protein was probed by tracking the emission wavelength at 360 nm, on excitation at 280 nm using a fluorescence spectrophotometer LS55 PerkinElmer.

Mammalian Cell Culture. Human cervical cancer (HeLa) and human embryonal kidney (HEK-293) cell lines were obtained from National Centre for Cell Sciences, Pune. Cells were maintained in Dulbecco's Modified Eagle's Medium (DMEM), containing 10% FBS, 100 U/mL penicillin, and 10 mg/mL streptomycin in humidified atmosphere at 37 °C in a 5% carbon dioxide incubator.

Stability Studies of NPs and Tracking the Release of Protein. The luminescence property of Au NCs was utilized for probing the stability of NPs and release of protein in culture media, over a span of 48 h. For this purpose, HeLa cells were seeded in six-well plates at a density of 10⁵ cells per well and allowed to attach for 8 h. Thereafter, media were replaced by serum-free media containing only NPs as well as NPs bound to GST-sFRP1 in separate wells. One set of NPs and protein bound NPs was collected at each time point in their culture media. Luminescence intensity was measured with Fluorolog-3, Horiba JobinYvon, USA, at 2 h, 14 h, 24 h, and 48 h.

Assessment of Cell Viability. The effect of sFRP1-NPs on HeLa cells was determined by the MTT (3-(4,5-dimethylthiazol-2-yl)-2,5-diphenyltetrazolium bromide) assay. HeLa cells were seeded in a 96-well plate at a density of 7000 cells per well. After allowing the cells to attach for 8 h, they were treated with Chi-Au NC-Alg NPs, GST-sFRP1, and sFRP1-NPs for 48 h. The activity of recombinant protein was also tested on noncancerous cell line HEK-293. Then, the MTT assay was performed, whereby MTT was converted to purple formazan crystals by healthy cells. These crystals were dissolved in dimethyl sulfoxide, and absorbance was recorded at 550 nm, with background reference measured at 655 nm. All concentrations were added in triplicate, and the experiment was performed three times. Cell viability was calculated using the following formula, and statistical tests were performed.

$$\% \text{ of cell viability} = \frac{(A_{550} - A_{655})_{\text{sample}}}{(A_{550} - A_{655})_{\text{control}}} \times 100$$

Tracking NPs with High-End Deconvolution Microscopy. Tracking the localization of NPs was essential to confirm whether they remained in the media or were taken up by the cells. For this purpose, they were viewed after incubation with sFRP1-NPs under high-end deconvolution microscope (DeltaVision, GE Healthcare Life Sciences).

Preparation of Whole Cell Protein Lysate and Western Blotting. Western blotting was done to analyze the signaling pathway responsible in bringing about the detrimental effects of GST-sFRP1 on the growth of HeLa cells. In particular, phosphorylation status of β -catenin protein, which is central to the Wnt pathway, was checked. Cells treated with protein-NPs were also analyzed in order to evaluate the functionality of protein in the two cases. With this intent, cells were treated with both for 24 h in 60 mm culture petridishes containing serum-free media. A control sample with cells incubated in serum-free media for 24 h was also kept. Thereafter, media were discarded, and cells were washed two times with phosphate buffered saline (PBS). RIPA buffer (Sigma-Aldrich) supplemented with protease inhibitor cocktail (Sigma-Aldrich) was added to each plate and incubated for 5 min at cold temperatures under mild shaking. The cell lysate was then sonicated for 10 s with a probe sonicator in ice. Thereafter, samples were centrifuged at 8000g for 10 min at 4 °C to pellet down the cell debris. The respective supernatants, containing all soluble proteins, were collected, and the amount of protein in each was quantified using Lowry's method of protein estimation. Then, equal amounts of all three samples (untreated, treated with protein, and treated with protein-NPs) were electrophoresed in triplicate on 12% SDS-PAGE (sodium dodecyl sulfate-polyacrylamide gel electrophoresis) and transferred to a PVDF membrane. Blocking of the membrane was done with 4% BSA (bovine serum albumin) in PBST (10 mM PBS with 0.1% Tween 20) for 2 h. It should be mentioned here that all steps followed for the detection of phosphorylated protein

require the usage of TBST (50 mM tris, 150 mM sodium chloride, and 0.1% Tween 20) instead of PBST. Eventually, the membrane was cut such that each replicate sample was incubated overnight with either of the primary antibodies against human β -catenin, the phosphorylated form of β -catenin (pSer³³/pSer³⁷), and β -actin as the endogenous control (Sigma-Aldrich). Next, the membrane was washed with PBST/TBST five times and incubated with the corresponding horseradish peroxidase labeled secondary antibodies (Sigma-Aldrich). Again, washing was done five times with PBST/TBST, before the blots were developed with Chemiluminiscent Peroxidase Substrate (Sigma-Aldrich).

Acridine Orange (AO)/Ethidium Bromide (EB) Dual Staining.

To distinguish between healthy and membrane compromised cells, cells were stained with AO and EB simultaneously. Cells were grown in a 96-well plate, as before. Recombinant protein, alone and after being bound to Chi-Au NC-Alg NPs, was added at concentrations at which the maximum effect was observed in the MTT assay. At the end of the treatment period of 48 h, media were discarded, cells were washed thoroughly with 10 mM PBS, and AO and EB were added at concentrations of 2 μ g/mL and 10 μ g/mL, respectively. After incubation for 5 min in dark, the cells were washed with fresh PBS and visualized under a fluorescence microscope (Nikon ECLIPSE TS100).

Expression Profiling for Downstream Genes. The expression of two genes, cyclin D1 and survivin, functioning downstream of β -catenin in the Wnt pathway, was also studied to further confirm the implication of this signaling pathway. RNA was isolated with the Tri reagent based method, and cDNA was synthesized with a RevertAid H-minus Reverse Transcriptase kit (Fermentas). A 220 bp fragment of the gene for cyclin-D1 was amplified from the cDNA using a forward primer 5'-CGCCCCACCCCTCCAG-3' and a reverse primer 5'-CGCCCAGACCCTCAGACT-3', whereas a 170 bp fragment of the survivin gene was amplified using the forward primer 5'-AGAACTGGCCCTTCTTGGAGG-3' and the reverse primer 5'-CTTTTATGTTCTCTATGGGGTC-3'.

Combination Therapy with Cisplatin. Cisplatin was also added in combination with the above samples to determine if the protein-NPs have the potential to induce sensitization of HeLa cells toward cisplatin. The MTT assay was conducted following the above protocol. The range of concentration of cisplatin used was 1 μ g/mL to 5 μ g/mL.

Cell Cycle Analysis. The effect of the protein conjugated NPs on the cell cycle pattern of HeLa cells was evaluated by Fluorescence Activated Cell Sorting (FACSCalibur, BD Biosciences, USA) using propidium iodide (PI). Also, its impact in combination with cisplatin was ascertained in the same manner. Cells were seeded at a density of 10^5 cells per well in a six-well plate and allowed to attach overnight. Thereafter, cells were treated separately with recombinant sFRP1 and sFRP1-NPs, alone and in combination with cisplatin. The concentration used for GST-sFRP1 was 10 nM, and an equivalent concentration of protein-NPs was used. The concentration of cisplatin used was 3 μ g/mL. All concentrations were decided based on the data obtained from MTT assays. Samples were treated for 48 h at the end of which cells were harvested by trypsinization and fixed with 70% ethanol in ice for 1 h. Then, they were centrifuged at 650g for 5 min at 4 °C. Pellets thus formed were washed with cold PBS before being incubated in 0.4 mg/mL RNase solution for 1 h at 37 °C. PI was added to each sample at a concentration of 10 μ g/mL and incubated in the dark until the time of analysis in FACSCalibur.

Detection of Apoptosis by Fluorescein Isothiocyanate (FITC) Conjugated Annexin V/PI. This assay was performed to distinguish among the healthy, early apoptotic, and late apoptotic cells, following treatment. HeLa cells were grown and treated following the same method as that described above. Cells were collected by trypsinization, washed with PBS, and stained with FITC-Annexin V and PI, following the manufacturer's protocol provided with the FITC Annexin V apoptosis detection kit (BD Biosciences). Finally, the cells were analyzed by FACS. All concentrations used were the same as those in the previous experiment.

RESULTS AND DISCUSSION

Recombinant GST-sFRP1 Bound to Chi-Au NC-Alg NPs.

The recombinant vector pGEX-4T2 with the cloned human sFRP1 was transformed into *E. coli* BL21(DE3). GST tagged sFRP1 protein was expressed and purified from the bacterial culture using an affinity chromatography column, which generated a discrete single band at 61 kDa corresponding to GST-sFRP1, in SDS-PAGE (Figure 1A). The pI (isoelectric

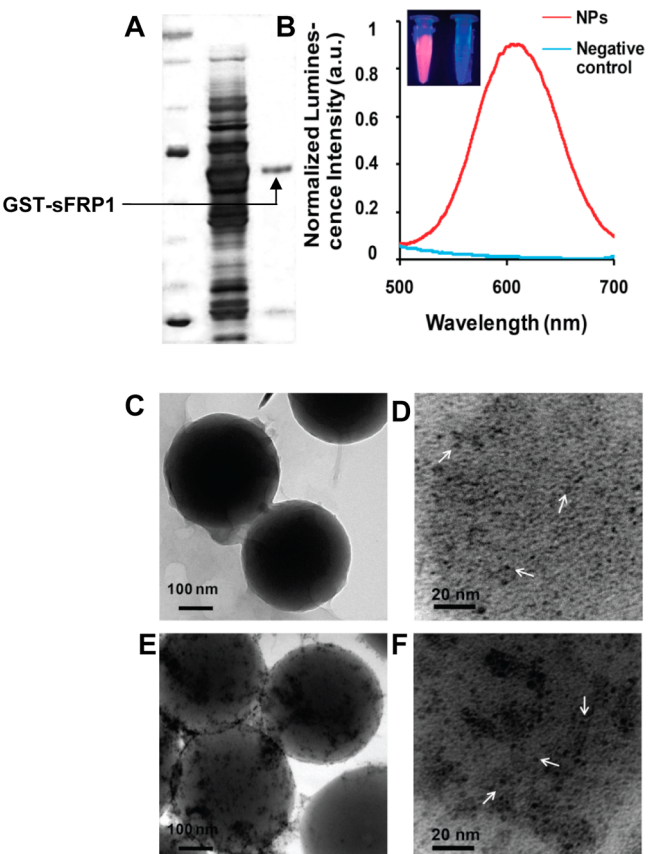


Figure 1. (A) 12% SDS-PAGE showed a single band of purified GST-sFRP1 at its legitimate size of 61 kDa. (B) Emission spectrum of Chi-Au NC-Alg NPs displaying bright luminescence when excited with 320 nm wavelength of light; negative control containing all the constituents of the NPs excepting gold chloride. (C) As-synthesized NPs were drop casted, dried, and imaged with TEM, which depicted spherical NPs of around 350 nm diameter. (D) Magnified image to show Au NCs. (E) Binding of NPs with protein was done in Tris buffer for 2 h. Thereafter, the sample was dried on a TEM grid and imaged. (F) Magnified image to show Au NCs after the binding of protein.

pH) of GST-sFRP1 calculated theoretically using an ExPASy pI calculator was found to be 8.73, which meant that the recombinant protein would have a net positive surface charge at physiological pH. Also, its mechanism of action requires its presence outside the cell, in the culture media, where it binds to Wnt ligands.⁴⁵ In noncancerous cells, sFRP1 is known to bind to Wnt ligands, which are extracellular secretory proteins, and prevent it from carrying out its downstream signaling.⁴⁶ In cancer cells, sFRP1 is downregulated,^{47,48} and hence, Wnt binds to its cell surface receptor frizzled (FZD) to transduce the Wnt cell signaling pathway, resulting in up-regulation of pro-proliferative genes like cyclin D1, survivin, and c-myc.

Exogenous addition of GST-sFRP1 to cervical cancer cells led to its binding to Wnt ligand in the extracellular medium.²¹ In order to overcome the limitations of treatment with recombinant protein alone, we formulated biocompatible composite NPs. Additionally, for real time monitoring of protein we incorporated luminescent Au NCs owing to their enhanced photophysical activity. Prior to the formation of the composite NPs, Au NCs were synthesized with gold(III) chloride, on biopolymer chitosan, in the presence of reducing agent 2-mercaptopropionic acid (MPA), based on the method developed earlier.³⁵ They were converted to NPs using biopolymer alginate, which being negatively charged at physiological pH, helped in the formation of spherical NPs by electrostatic interactions with positively charged amine groups of chitosan. As-synthesized composite NPs revealed characteristic emission of the Au NCs at 610 nm when excited by 320 nm UV light as depicted in Figure 1B. MALDI-TOF data showed a prominent peak at *m/z* equaling 5310.98 (shown in Supporting Information, Figure S1), which corresponds to $[Au_{20+} (MPA)_{12+} 5 Na^+]$. This was a confirmation of the organization of the gold cluster, comprising 20 gold atoms. The extinction spectrum of the synthesized NPs did not display any peak in the range of 400–800 nm, ruling out the possibility of the formation of SPR positive gold NPs^{32,35} (Figure S2).

The size and surface charge of the composite NPs were optimized by varying the concentration of chitosan to alginate ratio to attain bigger and negatively charged NPs, which possessed a reduced capability of penetrating the cell membrane. This was necessary as the recombinant protein binds to Wnt ligands in the extracellular medium to exert its activity. Average hydrodynamic diameter of the NPs was 599 nm (Figure S3A) and that of protein-NPs was 767 nm (Figure S3B), as analyzed by DLS. Zeta potential studies revealed that the positively charged chitosan Au NCs were converted to negatively charged NPs (-26.6 mV) by the addition of alginate (Figure S3C). Interaction of NPs with GST-sFRP1 caused a further reduction in its negative charge from -26.6 mV to -15.8 mV (Figure S3D). The negative charge of the NPs would eventually reduce the endocytic uptake of the protein-NP conjugate by the negatively charged cell membrane.⁴⁹ Besides, this decrease in negative charge may enhance the circulation time of the NPs by reducing the uptake by macrophages. Literature also suggests that positive NPs are cleared more quickly from the body by the mononuclear phagocyte system (MPS), as compared to neutral or negatively charged NPs.⁴⁹ It may be emphasized here that the features of size and surface charge tunability of the composite NPs greatly widen the scope of their clinical application.

TEM images revealed the formation of nearly uniform spherical NPs of an average diameter of $320 \pm 15\text{ nm}$ (Figure 1D), with the size distribution profile shown in Figure S4. The difference in size of NPs as observed in TEM images, showing dried samples, and DLS analysis, with samples in solution, was probably due to the swelling of NPs in solution. Both chitosan and alginate have been reported to swell in aqueous solution, depending on their concentration and degree of cross-linking.⁵⁰ The Au NCs are clearly visible in the magnified image (Figure 1E). Interestingly, the composite NPs remained intact even after interaction with protein (Figure 1F and G), which implied that the protein structure did not interfere with the chemistry of the NPs. This finding is quite remarkable as it unveils the potential of this system for the delivery of therapeutic proteins in the future.

Another important necessity for drug or protein delivery is the tracking of its path after its administration. The extraordinary luminescence properties of the Au NCs in the composite NPs enable its use as a luminescent probe for imaging and tracking purposes.³¹ The quantum yield was calculated to be 1.3%, using quinine sulfate as standard (details are given in Supporting Information). Furthermore, epifluorescence microscopy showed discrete particles displaying green and red images with blue and green filters, respectively (Figure S5). This fascinating feature can be exploited for optical imaging studies, especially if more than one fluorescent molecule is required for any experiment. Also, previous investigations have demonstrated that Au NCs undergo photobleaching to a far lesser degree than organic dyes, which further enriches the credibility of Au NCs.^{31,35}

Binding and Release Studies of Recombinant Protein.

Binding studies of the GST-sFRP1 were conducted by probing the luminescence of Au NCs. Maximum binding efficiency was calculated to be approximately 70.6% in Tris buffer at pH 7.4 (Figure 2A and B). Binding of protein to NPs was further substantiated by Fourier transform infrared (FTIR) spectroscopy (Figure S6) and circular dichroism spectral analysis. In the FTIR spectra, the binding of protein to Chi-Au NC-Alg NPs was represented by a shift in the characteristic peak for amide I from 1609 to 1613 cm^{-1} , with the appearance of a second peak at 1524 cm^{-1} signifying amide II. Circular dichroism analysis was performed to study the conformational change of protein after binding with NPs. In a previous study, we had reported that α -helical structures and β -sheets of GST-sFRP1 were 20.7% and 33.5%, respectively.²¹ Upon binding to NPs, the α -helix was found to reduce to 9.3%, and β -sheets were increased to 60.6% (Figure S7). This indicated that although the protein underwent some conformational change upon binding to NPs, its secondary structures were intact to a significant extent. Subsequent experiments confirmed that the functionality of the protein was retained.

The release profile of GST-sFRP1 from Chi-Au NC-Alg NPs was examined in PBS (pH 7.4) by probing the intrinsic luminescence of protein. It demonstrated a sustained release of about 40% of the bound protein from composite NPs after 48 h (Figure 2C). It can be anticipated that bound protein may also interact with its target, i.e., the Wnt ligand through protein–protein interaction in the extracellular media and generate the desired cell inhibitory effects. The sustained release profile obtained in this case is ideal for prolonged activity of the protein.

Stability of Au NCs in Cell Culture Media Studied by Probing Luminescence. As an *in vitro/in vivo* biological system contains an assortment of proteins, the stability of the protein-NPs in cell culture media was also investigated by probing the luminescence of Au NCs. In this pursuit, luminescence of the NPs was quenched by 20% in the initial hours possibly due to the instability of the NPs (in absence of protein) in media (Figure 2D). However, interaction of the NPs with different components of the medium, such as amino acids, resulted in the stabilization and constancy of the luminescence due to Au NCs over longer period of time. However, interaction of the protein with NPs significantly stabilized the NPs, and the luminescence intensity remained undiminished, where the emission intensities due to both bound and unbound NPs were normalized to emphasize the difference in their stability. Figure S8 depicts that the binding of protein to NPs in culture media quenched the luminescence of

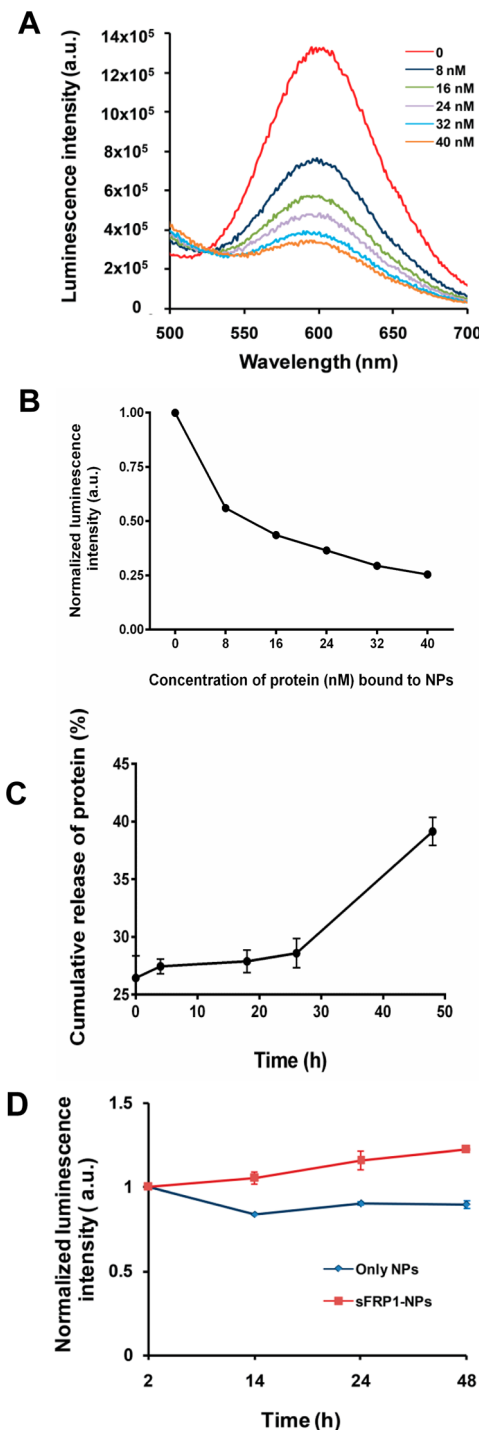


Figure 2. (A and B) Binding of NPs with increasing concentrations of protein was done for 2 h in Tris buffer (pH 7.4). Probing the luminescence of Au NCs yielded protein concentration dependent quenching of luminescence, with a maximum binding efficiency of 70.6% for a protein concentration of 32 nm, after which saturation was attained. (C) After 2 h of binding of NPs with protein in Tris, a time dependent release profile was investigated in PBS buffer (pH 7.4), which illustrated a maximum of 40% release of bound protein from the NPs in 48 h. (D) Stability studies in growth media displayed enhanced stability of the protein-NPs, as compared to unbound NPs. For this experiment, cells were treated with NPs, with or without bound protein, and the culture media were collected for analysis of luminescence, at different time points up to 48 h.

the clusters, corroborating the results obtained from the binding studies in Tris buffer at pH 7.4. However, maximum luminescence quenching was observed at 2 h, which decreased gradually in a time dependent fashion. This may prove to be an excellent tool to perform relative quantification studies using stable and labeled payload *in vitro*, by using Au NCs as luminescent probes.⁵¹

Tracking NPs for Anticancer Function. Researchers have reported that transfection of the sFRP1 gene in mammalian cancer cells leads to reduced cell growth and proliferation.^{19,20} We have also shown previously the inhibitory effects of GST-sFRP1 on cancer cell lines.²¹ In this study, we have established that the protein after being bound to NPs not only retained its functionality but also displayed improved cell inhibitory effect, as compared to those of protein alone. This can be attributed to the stability and sustained release of protein from the NPs, resulting in the prolonged presence of functional sFRP1 in the medium, as compared to that in the protein alone. Cell viability was reduced to 50% for protein-NPs, while the corresponding concentration of protein (12 nM) showed a viability of 61% (Figure 3A). Composite NPs were found to be completely nontoxic even at high concentrations, making them ever more suitable for clinical applications in tracking and delivery of cargos. Moreover, GST-sFRP1 did not exert any inhibitory action on noncancerous cell line HEK-293 (Figure S9). This would imply reduced side effects, making this protein ideal for cancer therapy.

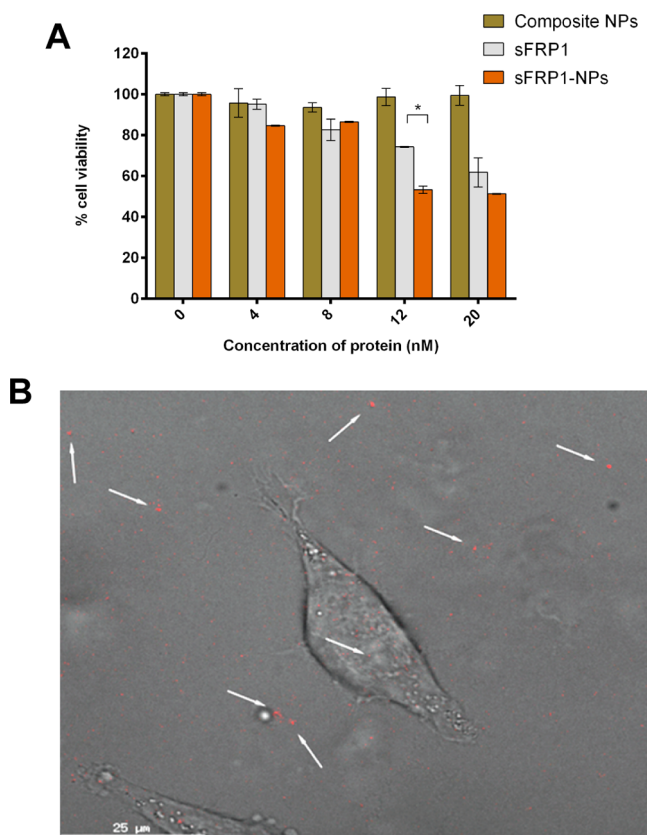


Figure 3. (A) Treatment with protein-NPs showed profound effect on the viability of HeLa cells, compared to that of protein alone, as deduced from the cell viability assay. Cells were also treated with NPs of corresponding concentrations. (B) Imaging NPs in cell culture media showed that they remained in the media and were not taken up by cells at 2 h.

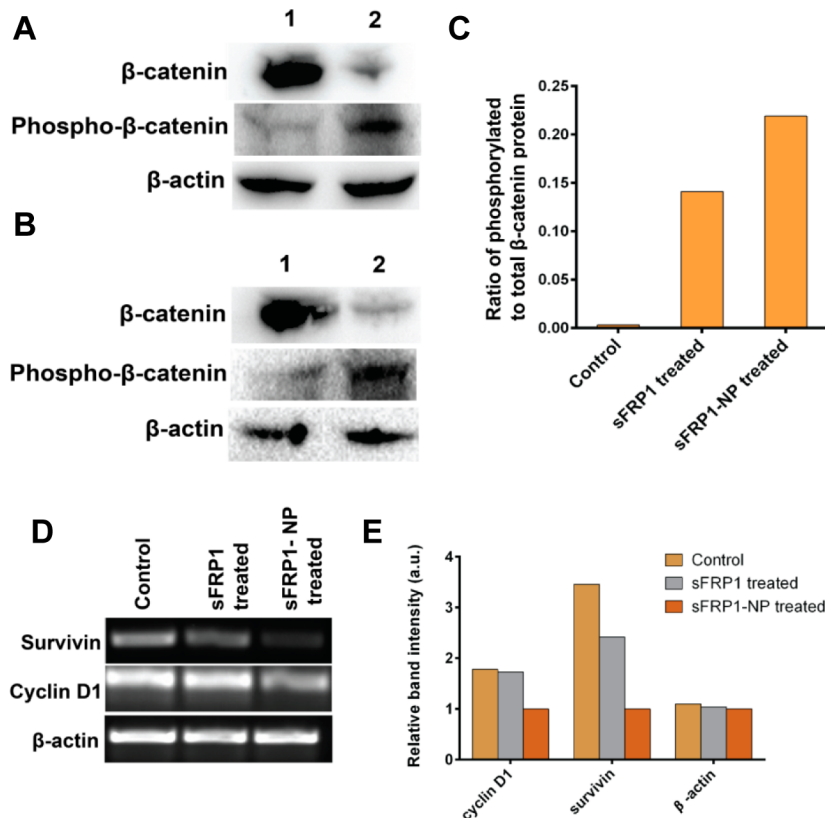


Figure 4. Western blotting to detect β -catenin, phosphorylated β -catenin, and β -actin protein levels in HeLa cells. (A) Lane-1, untreated control; lane 2, treated with sFRP1 for 24 h. (B) Lane-1, untreated control; lane 2, treated with sFRP1-NPs for 24 h. (C) Graphical representation of fold change in a ratio of phosphorylated β -catenin to β -catenin protein. (D) Expression analysis of downstream survivin and cyclin D1 genes in cells treated with sFRP1 and sFRP1-NPs for 24 h, as compared to that of untreated cells. (E) Graphical representation of fold change of cyclin D1, survivin, and β -actin.

Herein, it should be mentioned that sFRP1 exerts its activity in the extracellular medium. To determine the fate of NPs, the particles were tracked using a deconvolution microscope at 60 \times magnification (Figure 3B). The images clearly deciphered that NPs remained in media with red luminescence, and thus, our criteria for synthesizing the NPs were met. This was corroborated by flow cytometry based quantitative analysis (details provided in Supporting Information, along with Figure S10).

Targeting the Wnt Signaling Pathway. The downstream Wnt pathway was studied to elucidate the mechanism of the growth inhibitory effect of recombinant sFRP1 on HeLa cells and to prove that the Wnt pathway was indeed being targeted by the sFRP1-NPs. As sFRP1 is reported to block Wnt pathway in normal adult cells, we focused on the expression profile of a few crucial molecules of the Wnt cascade. The most prominent member lying downstream of Wnt is the β -catenin protein. In cancer cells, the Wnt pathway is active, where β -catenin is stabilized by several proteins and accumulates in the cytoplasm. Subsequently, it translocates into the nucleus and transcriptionally upregulates the expression of certain pro-proliferative genes like cyclin D1 and survivin. In presence of active sFRP1 in normal cells, β -catenin is phosphorylated to mark it for degradation by ubiquitination, and expressions of cyclin D1 and survivin are decreased. Hence, the β -catenin protein level as well as gene expression of cyclin D1 and survivin were examined by Western blotting and semiquantitative PCR, respectively. For Western blotting, 53 μ g of whole cell protein from each of three samples (control, GST-sFRP1, and Chi-Au

NC-Alg conjugated GST-sFRP1) was loaded into each well of a 12% SDS-PAGE, after quantifying them with the Lowry assay. β -Actin was used as the loading control for all samples. β -Catenin was significantly down-regulated, and phosphorylated β -catenin was significantly upregulated in both sFRP1 (Figure 4A) and sFRP1-NP treated cells (Figure 4B), as compared to the control cells. Ratio of phosphorylated to total β -catenin was negligible in control cells, whereas it increased 47-fold and 73-fold in protein and protein-NP treated cells, respectively (represented graphically in Figure 4C). Gene expression levels decreased for cyclin D1 (1.03 times and 1.78 times for protein and protein-NPs, respectively). Similarly, the expression of the survivin gene also decreased (1.43-fold and 3.45-fold, respectively), as illustrated in Figure 4D. Graphical representation of fold-change in gene expression is given Figure 4E. These experiments provided conclusive evidence that GST-sFRP1 exerted its anticancer effect by targeting the Wnt pathway. Also, they confirmed that the recombinant protein entirely retained its functional integrity after being bound to Chi-Au NC-Alg NPs.

Furthermore, visualization in epi-fluorescence microscopy upon dual staining with acridine orange (AO) and ethidium bromide (EB) demonstrated that treatment with GST-sFRP1 triggered membrane damage of cells. The effect was enhanced on treatment with sFRP1-NPs, where a significant population of the cells showed staining with AO and EB. Details and a figure have been furnished in Supporting Information (Figure S11). Hence, we can surmise that the sFRP1-NPs successfully damaged cancer cells by targeting the Wnt cascade.

Molecular Mechanisms in a Combination Module. Studies have elaborated on the phenomenon of chemosensitization of cancer cells toward a conventional chemotherapeutic agent by overexpression of a relevant gene⁵² or addition of a therapeutic protein.^{37,40} This fact has been exploited in this work, whereby the binding of protein to Chi-Au NC-Alg was found to considerably sensitize HeLa cells toward cisplatin. The MTT assay exhibited a sharp reduction in cell viability in the case of combination therapy (cisplatin with protein-NPs), as compared to that of only protein-NPs or only cisplatin treated cells (Figure 5A). The concept of combination therapy, such as chemotherapy followed by radiotherapy, has been prevalent for decades.^{53,54} Although this mode of treatment has accomplished some degree of success in certain types of cancers,^{55–57} the aftermath concerning exacerbated side effects and the development of resistance are yet to be addressed. Hence, the module of cotherapy that we have demonstrated, combining protein therapeutics with chemotherapy, provide a new facet to our work. It has the potential to augment the efficacy, reduce side effects, and avoid the development of resistance, thereby outweighing the benefits of monotherapy⁵⁸ or prevalent combination therapies.

To investigate the mode of impact of the protein-NP conjugate on the cell cycle progression of HeLa cells, flow cytometric analysis with PI was conducted. PI is a DNA intercalating agent that is employed to measure DNA content of cells, which in turn, indicates the phase of the cell cycle. Treatment of HeLa cells with a low concentration of protein (10 nM), bound to NPs or otherwise, induced a slight increase in the G2/M phase and a decrease in the G1 phase. In combination with cisplatin (3 µg/mL), the G2/M population of cells treated with protein-NPs combined with cisplatin increased dramatically, the increase being over 1.5-fold (42%) as compared to that of only cisplatin treated cells (27%), depicting a G2/M arrest (Figure 5B). A prominent sub G1 population (5.4%) was also observed, indicating apoptosis. Cisplatin has been previously reported to arrest cells in G2/M phase of the cell cycle.⁵⁹ However, we attributed the significantly enhanced efficacy of cotherapy to the blockage of the Wnt pathway by the sFRP1-NPs. As the Wnt cascade plays a prominent role in cell proliferation, disrupting the pathway by the sFRP1-NPs possibly sensitizes the cancer cells to treatment with chemotherapy. Correlating with the results obtained in the MTT assay, it can be concluded that even a low concentration of sFRP1-NPs is sufficient to greatly sensitize the cancer cells toward cisplatin.

For the detection of the mechanism of cell death, cells were stained with FITC Annexin V and counter-stained with PI. FITC Annexin V stains the cells by labeling phosphatidylserine sites on the cell membrane in early or late apoptotic stage, prior to the complete loss of cytoplasm. PI stains cells with the damaged membrane as it is cell impermeable, staining late apoptotic or necrotic cells. This difference forms the basis of the assay for the detection of apoptosis. Early apoptotic cells are Annexin V-FITC positive, whereas late apoptotic cells are positive for both dyes. This FACS based experiment showed that the percentage of live cells decreased (from 92% in control to 75% in treated) and that late apoptotic cells increased (from 6% in control to 22% in treated) substantially upon treatment with GST-sFRP1 (10 nM)-NPs. These data were found to be completely in agreement with the dual staining results with AO and EB observed previously. Moreover, this effect was augmented greatly in case of combination therapy (49% live

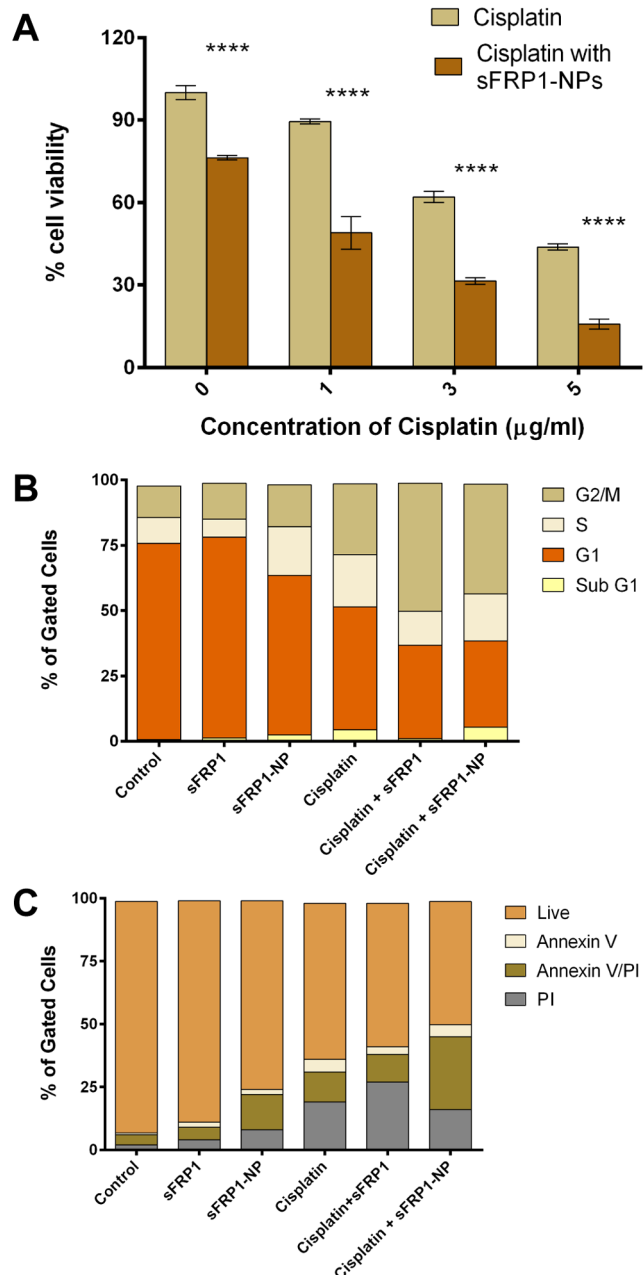


Figure 5. (A) MTT assay showing the viability of HeLa cells after combination therapy of protein-NPs with cisplatin for 48 h. (B) Cell cycle analysis of HeLa cells of control and treated cells by FACS, performed 48 h after treatment with sFRP1, sFRP1-NPs, and their respective combination with cisplatin. (C) FITC Annexin V/PI staining of HeLa cells showing a decrease in population of live cells in samples treated for 48 h, with respect to untreated control cells.

and 45% late apoptotic) of protein-NPs and cisplatin, as opposed to either of them alone (Figure 5C). Although, protein alone did not exhibit a significant difference with control cells, combination therapy with cisplatin yielded a high population of late apoptotic cells. These results corroborated our previous observations and proved that the above treatments enforce the apoptotic mode of cell death. Chemosensitization of HeLa cells mediated by cotherapy of sFRP1-NPs and cisplatin is a novel mode of targeting two different pathways for treating cancer.

CONCLUSIONS

In this study, we have succeeded in engineering a system comprising recombinant therapeutic protein bound to novel NPs embedded with highly fluorescent gold nanoclusters. The luminescence properties of Au NCs were exploited for the purpose of tracking, imaging, and profiling the release of protein from NPs. Features of the composite NPs were effectively modulated to meet the criteria of protein binding, release, and its function. Also, GST-sFRP1 was delivered in its functionally active form and exerted its anticancerous activities on HeLa cells by blocking the Wnt signal cascade. Interaction of protein with the NPs considerably augmented its efficiency. Herein, we fabricated a nanosystem ensemble to target and simultaneously block a signaling pathway specific to cancer, making this study a first of its kind. Moreover, combination of sFRP1-NPs and traditional drug cisplatin demonstrated sensitization of the cancer cells toward cisplatin, providing a novel regime of cotherapy. Cell based assays, dual staining methods, and apoptosis detection experiments provided detailed characteristics of the mode of cell death. The results obtained distinctly exhibited that cotherapy caused significantly greater damage to cancer cells than chemotherapy or NP mediated protein therapy alone. Hereby, we targeted two different pathways, the Wnt pathway playing a prominent role in cancer and the established apoptotic induction by cisplatin.⁶⁰ Hence, it paves a new path of generating composite nanoparticles to modulate signaling mechanisms, which reduces the required dosage of chemotherapeutic drugs by aiming at two independent pathways for the remedy of cancer. It can be concluded that these biocompatible and nontoxic NPs may prove to be archetypical for tracking and sustained release of functionally active therapeutic sFRP1 for blocking Wnt signals, which holds immense prospect in cancer theranostics.

ASSOCIATED CONTENT

Supporting Information

The Supporting Information is available free of charge on the ACS Publications website at DOI: [10.1021/acsbiomaterials.5b00305](https://doi.org/10.1021/acsbiomaterials.5b00305).

UV-visible spectra of NPs; DLS; zeta potential studies; size distribution profile of nanoparticles; calculation of quantum yield; fluorescence emitted in two different filters by nanoparticles under a microscope; FTIR spectra; circular dichroism spectra of sFRP1 after binding to NPs; fluorescence quenching of NPs in media; after binding to sFRP1; cell viability assay after treatment of noncancerous cell line HEK-293 with sFRP1; and dual staining of cervical cancer cells (HeLa) with acridine orange and ethidium bromide to demonstrate apoptosis ([PDF](#))

AUTHOR INFORMATION

Corresponding Author

*Phone: +0361-258-2206. Fax: +0361-258-2249. E-mail: sghosh@iitg.ernet.in.

Notes

The authors declare no competing financial interest.

ACKNOWLEDGMENTS

We acknowledge the Department of Biotechnology and the Department of Electronics and Information Technology (No.

S(9)/2012-NANO (Vol. II)), Government of India for financial support. We also acknowledge the help of Central Instruments Facility (CIF) and the Centre for Nanotechnology, IIT Guwahati, as well as GE Healthcare.

REFERENCES

- Zhen, Z.; Tang, W.; Chen, H.; Lin, X.; Todd, T.; Wang, G.; Cowger, T.; Chen, X.; Xie, J. RGD-Modified Apoferritin Nanoparticles for Efficient Drug Delivery to Tumors. *ACS Nano* **2013**, *7*, 4830–4837.
- Gu, Z.; Biswas, A.; Zhao, M.; Tang, Y. Tailoring nanocarriers for intracellular protein delivery. *Chem. Soc. Rev.* **2011**, *40*, 3638–3655.
- Ramu, A.; Glaubiger, D.; Fuks, Z. Reversal of Acquired Resistance to Doxorubicin in P388 Murine Leukemia Cells by Tamoxifen and Other Triparanol Analogues. *Cancer Res.* **1984**, *44*, 4392–4395.
- O'Brien, M. E. R.; Wigler, N.; Inbar, M.; Rosso, R.; Grischke, E.; Santoro, A.; Catane, R.; Kieback, D. G.; Tomczak, P.; Ackland, S. P.; Orlandi, F.; Mellars, L.; Allard, L.; Tendler, C. Reduced cardiotoxicity and comparable efficacy in a phase III trial of pegylated liposomal doxorubicin HCl (CAELYX/Doxil®) versus conventional doxorubicin for first-line treatment of metastatic breast cancer. *Annals of Oncology* **2004**, *15*, 440–449.
- Florea, A.-M.; Büsselfberg, D. Cisplatin as an Anti-Tumor Drug: Cellular Mechanisms of Activity, Drug Resistance and Induced Side Effects. *Cancers* **2011**, *3*, 1351–1371.
- Mathé, G.; Amiel, J. L.; Schwarzenberg, L.; Schneider, M.; Cattan, A.; Schlumberger, J. R.; Hayat, M.; De Vassal, F. ACTIVE IMMUNOTHERAPY FOR ACUTE LYMPHOBLASTIC LEUKÆMIA. *Lancet* **1969**, *293*, 697–699.
- Rosenberg, S. A. IL-2: the first effective immunotherapy for human cancer. *J. Immunol.* **2014**, *192*, 5451–8.
- Chacon, J. A.; Sarnai, A. A.; Chen, J. Q.; Creasy, C.; Kale, C.; Robinson, J.; Weber, J.; Hwu, P.; Pilon-Thomas, S.; Radvanyi, L. Manipulating the tumor microenvironment ex vivo for enhanced expansion of tumor-infiltrating lymphocytes for adoptive cell therapy. *Clin. Cancer Res.* **2015**, *21*, 611–21.
- Giles, R. H.; van Es, J. H.; Clevers, H. Caught up in a Wnt storm: Wnt signaling in cancer. *Biochim. Biophys. Acta, Rev. Cancer* **2003**, *1653*, 1–24.
- Anastas, J. N.; Moon, R. T. WNT signalling pathways as therapeutic targets in cancer. *Nat. Rev. Cancer* **2013**, *13*, 11–26.
- Lee, A. Y.; He, B.; You, L.; Dadfarman, S.; Xu, Z.; Mazieres, J.; Mikami, I.; McCormick, F.; Jablons, D. M. Expression of the secreted frizzled-related protein gene family is downregulated in human mesothelioma. *Oncogene* **2004**, *23*, 6672–6.
- Suzuki, H.; Gabrielson, E.; Chen, W.; Anbazhagan, R.; van Engeland, M.; Weijenberg, M. P.; Herman, J. G.; Baylin, S. B. A genomic screen for genes upregulated by demethylation and histone deacetylase inhibition in human colorectal cancer. *Nat. Genet.* **2002**, *31*, 141–9.
- Marsit, C. J.; Karagas, M. R.; Andrew, A.; Liu, M.; Danaee, H.; Schned, A. R.; Nelson, H. H.; Kelsey, K. T. Epigenetic inactivation of SFRP genes and TP53 alteration act jointly as markers of invasive bladder cancer. *Cancer Res.* **2005**, *65*, 7081–5.
- Hu, E.; Zhu, Y.; Fredrickson, T.; Barnes, M.; Kelsell, D.; Beeley, L.; Brooks, D. Tissue restricted expression of two human Frzbs in preadipocytes and pancreas. *Biochem. Biophys. Res. Commun.* **1998**, *247*, 287–93.
- Caldwell, G. M.; Jones, C.; Gensberg, K.; Jan, S.; Hardy, R. G.; Byrd, P.; Chughtai, S.; Wallis, Y.; Matthews, G. M.; Morton, D. G. The Wnt antagonist sFRP1 in colorectal tumorigenesis. *Cancer Res.* **2004**, *64*, 883–8.
- Veeck, J.; Niederacher, D.; An, H.; Klopocki, E.; Wiesmann, F.; Betz, B.; Galm, O.; Camara, O.; Durst, M.; Kristiansen, G.; Huszka, C.; Knuchel, R.; Dahl, E. Aberrant methylation of the Wnt antagonist SFRP1 in breast cancer is associated with unfavourable prognosis. *Oncogene* **2006**, *25*, 3479–88.

- (17) Takada, T.; Yagi, Y.; Maekita, T.; Imura, M.; Nakagawa, S.; Tsao, S. W.; Miyamoto, K.; Yoshino, O.; Yasugi, T.; Takeuchi, Y.; Ushijima, T. Methylation-associated silencing of the Wnt antagonist SFRP1 gene in human ovarian cancers. *Cancer Sci.* **2004**, *95*, 741–4.
- (18) Fukui, T.; Kondo, M.; Ito, G.; Maeda, O.; Sato, N.; Yoshioka, H.; Yokoi, K.; Ueda, Y.; Shimokata, K.; Sekido, Y. Transcriptional silencing of secreted frizzled related protein 1 (SFRP 1) by promoter hypermethylation in non-small-cell lung cancer. *Oncogene* **2005**, *24*, 6323–7.
- (19) Yang, Z. Q.; Liu, G.; Bollig-Fischer, A.; Haddad, R.; Tarca, A. L.; Ethier, S. P. Methylation-associated silencing of SFRP1 with an 8p11–12 amplification inhibits canonical and non-canonical WNT pathways in breast cancers. *Int. J. Cancer* **2009**, *125*, 1613–21.
- (20) Shih, Y. L.; Hsieh, C. B.; Lai, H. C.; Yan, M. D.; Hsieh, T. Y.; Chao, Y. C.; Lin, Y. W. SFRP1 suppressed hepatoma cells growth through Wnt canonical signaling pathway. *Int. J. Cancer* **2007**, *121*, 1028–35.
- (21) Ghoshal, A.; Ghosh, S. S. Expression, Purification, and Therapeutic Implications of Recombinant sSFRP1. *Appl. Biochem. Biotechnol.* **2015**, *175*, 2087–103.
- (22) Richardson, T. P.; Murphy, W. L.; Mooney, D. J. Polymeric delivery of proteins and plasmid DNA for tissue engineering and gene therapy. *Crit. Rev. Eukaryotic Gene Expression* **2001**, *11*, 47–58.
- (23) Singh, A. K.; Hahn, M. A.; Gutwein, L. G.; Rule, M. C.; Knapik, J. A.; Moudgil, B. M.; Grobmyer, S. R.; Brown, S. C. Multi-dye theranostic nanoparticle platform for bioimaging and cancer therapy. *Int. J. Nanomed.* **2012**, *7*, 2739–2750.
- (24) Bardhan, R.; Lal, S.; Joshi, A.; Halas, N. J. Theranostic Nanoshells: From Probe Design to Imaging and Treatment of Cancer. *Acc. Chem. Res.* **2011**, *44*, 936–946.
- (25) Ghosh, R.; Goswami, U.; Ghosh, S. S.; Paul, A.; Chattopadhyay, A. Synergistic Anticancer Activity of Fluorescent Copper Nanoclusters and Cisplatin Delivered through a Hydrogel Nanocarrier. *ACS Appl. Mater. Interfaces* **2015**, *7*, 209–22.
- (26) Ma, L. L.; Feldman, M. D.; Tam, J. M.; Paranjape, A. S.; Cheruku, K. K.; Larson, T. A.; Tam, J. O.; Ingram, D. R.; Paramita, V.; Villard, J. W.; Jenkins, J. T.; Wang, T.; Clarke, G. D.; Asmis, R.; Sokolov, K.; Chandrasekar, B.; Milner, T. E.; Johnston, K. P. Small multifunctional nanoclusters (nanoroses) for targeted cellular imaging and therapy. *ACS Nano* **2009**, *3*, 2686–96.
- (27) Bian, P.; Zhou, J.; Liu, Y.; Ma, Z. One-step fabrication of intense red fluorescent gold nanoclusters and their application in cancer cell imaging. *Nanoscale* **2013**, *5*, 6161–6.
- (28) Shiang, Y.-C.; Huang, C.-C.; Chen, W.-Y.; Chen, P.-C.; Chang, H.-T. Fluorescent gold and silver nanoclusters for the analysis of biopolymers and cell imaging. *J. Mater. Chem.* **2012**, *22*, 12972–12982.
- (29) Tian, D.; Qian, Z.; Xia, Y.; Zhu, C. Gold Nanocluster-Based Fluorescent Probes for Near-Infrared and Turn-On Sensing of Glutathione in Living Cells. *Langmuir* **2012**, *28*, 3945–3951.
- (30) Retnakumari, A.; Setua, S.; Menon, D.; Ravindran, P.; Muhammed, H.; Pradeep, T.; Nair, S.; Koyakutty, M. Molecular-receptor-specific, non-toxic, near-infrared-emitting Au cluster-protein nanoconjugates for targeted cancer imaging. *Nanotechnology* **2010**, *21*, 055103.
- (31) Wu, X.; He, X.; Wang, K.; Xie, C.; Zhou, B.; Qing, Z. Ultrasmall near-infrared gold nanoclusters for tumor fluorescence imaging in vivo. *Nanoscale* **2010**, *2*, 2244–9.
- (32) Wang, C.; Li, J.; Amatore, C.; Chen, Y.; Jiang, H.; Wang, X.-M. Gold Nanoclusters and Graphene Nanocomposites for Drug Delivery and Imaging of Cancer Cells. *Angew. Chem., Int. Ed.* **2011**, *50*, 11644–11648.
- (33) Lin, C.-A. J.; Yang, T.-Y.; Lee, C.-H.; Huang, S. H.; Sperling, R. A.; Zanella, M.; Li, J. K.; Shen, J.-L.; Wang, H.-H.; Yeh, H.-I.; Parak, W. J.; Chang, W. H. Synthesis, Characterization, and Bioconjugation of Fluorescent Gold Nanoclusters toward Biological Labeling Applications. *ACS Nano* **2009**, *3*, 395–401.
- (34) Bian, P.; Zhou, J.; Liu, Y.; Ma, Z. One-step fabrication of intense red fluorescent gold nanoclusters and their application in cancer cell imaging. *Nanoscale* **2013**, *5*, 6161–6166.
- (35) Sahoo, A. K.; Banerjee, S.; Ghosh, S. S.; Chattopadhyay, A. Simultaneous RGB Emitting Au Nanoclusters in Chitosan Nanoparticles for Anticancer Gene Theranostics. *ACS Appl. Mater. Interfaces* **2014**, *6*, 712–724.
- (36) Zhang, X.-D.; Chen, J.; Luo, Z.; Wu, D.; Shen, X.; Song, S.-S.; Sun, Y.-M.; Liu, P.-X.; Zhao, J.; Huo, S.; Fan, S.; Fan, F.; Liang, X.-J.; Xie, J. Radiosensitizers: Enhanced Tumor Accumulation of Sub-2 nm Gold Nanoclusters for Cancer Radiation Therapy (Adv. Healthcare Mater. 1/2014). *Adv. Healthcare Mater.* **2014**, *3*, 152–152.
- (37) Zhang, A.; Tu, Y.; Qin, S.; Li, Y.; Zhou, J.; Chen, N.; Lu, Q.; Zhang, B. Gold nanoclusters as contrast agents for fluorescent and X-ray dual-modality imaging. *J. Colloid Interface Sci.* **2012**, *372*, 239–44.
- (38) Chen, A. M.; Zhang, M.; Wei, D.; Stueber, D.; Taratula, O.; Minko, T.; He, H. Co-delivery of Doxorubicin and Bcl-2 siRNA by Mesoporous Silica Nanoparticles Enhances the Efficacy of Chemotherapy in Multidrug-Resistant Cancer Cells. *Small* **2009**, *5*, 2673–2677.
- (39) Solal-Célyny, P.; Lepage, E.; Brousse, N.; Tendler, C. L.; Brice, P.; Haïoun, C.; Gabarre, J.; Pignon, B.; Tertian, G.; Bouabdallah, R.; Rossi, J. F.; Doyen, C.; Coiffier, B. Doxorubicin-containing regimen with or without interferon alfa-2b for advanced follicular lymphomas: final analysis of survival and toxicity in the Groupe d'Etude des Lymphomes Folliculaires 86 Trial. *J. Clin. Oncol.* **1998**, *16*, 2332–8.
- (40) Banerjee, S.; Sahoo, A. K.; Chattopadhyay, A.; Ghosh, S. S. Hydrogel nanocarrier encapsulated recombinant I[small kappa]B-[small alpha] as a novel anticancer protein therapeutics. *RSC Adv.* **2013**, *3*, 14123–14131.
- (41) Cho, K.; Wang, X.; Nie, S.; Chen, Z.; Shin, D. M. Therapeutic Nanoparticles for Drug Delivery in Cancer. *Clin. Cancer Res.* **2008**, *14*, 1310–1316.
- (42) Leamon, C. P.; Reddy, J. A. Folate-targeted chemotherapy. *Adv. Drug Delivery Rev.* **2004**, *56*, 1127–41.
- (43) Qian, Z. M.; Li, H.; Sun, H.; Ho, K. Targeted drug delivery via the transferrin receptor-mediated endocytosis pathway. *Pharmacol. Rev.* **2002**, *54*, 561–87.
- (44) Lakowicz, J. R. *Principles of Fluorescence Spectroscopy*; Springer: New York, 2006; pp 54–55.
- (45) Surana, R.; Sikka, S.; Cai, W.; Shin, E. M.; Warrier, S. R.; Tan, H. J.; Arfuso, F.; Fox, S. A.; Dharmarajan, A. M.; Kumar, A. P. Secreted frizzled related proteins: Implications in cancers. *Biochim. Biophys. Acta, Rev. Cancer* **2014**, *1845*, 53–65.
- (46) Ugolini, F.; Charafe-Jauffret, E.; Bardou, V. J.; Geneix, J.; Adelaïde, J.; Labat-Moleur, F.; Penault-Llorca, F.; Longy, M.; Jacquemier, J.; Birnbaum, D.; Pebusque, M. J. WNT pathway and mammary carcinogenesis: loss of expression of candidate tumor suppressor gene SFRP1 in most invasive carcinomas except of the medullary type. *Oncogene* **2001**, *20*, 5810–7.
- (47) Liu, C.; Li, N. A. N.; Lu, H.; Wang, Z.; Chen, C.; Wu, L. I. N.; Liu, J.; Lu, Y.; Wang, F. Circulating SFRP1 promoter methylation status in gastric adenocarcinoma and esophageal squamous cell carcinoma. *Biomed. Rep.* **2015**, *3*, 123–127.
- (48) Ricketts, C. J.; Hill, V. K.; Linehan, W. M. Tumor-Specific Hypermethylation of Epigenetic Biomarkers, Including SFRP1, Predicts for Poorer Survival in Patients from the TCGA Kidney Renal Clear Cell Carcinoma (KIRC) Project. *PLoS One* **2014**, *9*, e85621.
- (49) Albanese, A.; Tang, P. S.; Chan, W. C. The effect of nanoparticle size, shape, and surface chemistry on biological systems. *Annu. Rev. Biomed. Eng.* **2012**, *14*, 1–16.
- (50) Remuñán-López, C.; Bodmeier, R. Mechanical, water uptake and permeability properties of crosslinked chitosan glutamate and alginate films. *J. Controlled Release* **1997**, *44*, 215–225.
- (51) Le Guevel, X.; Daum, N.; Schneider, M. Synthesis and characterization of human transferrin-stabilized gold nanoclusters. *Nanotechnology* **2011**, *22*, 275103.
- (52) Vernejoul, F.; Ghenassis, L.; Souque, A.; Lulka, H.; Drocourt, D.; Cordelier, P.; Pradayrol, L.; Pyronnet, S.; Buscail, L.; Tiraby, G. Gene Therapy Based on Gemcitabine Chemosensitization Suppresses Pancreatic Tumor Growth. *Mol. Ther.* **2006**, *14*, 758–767.

- (53) Fine, H. A.; Dear, K. B. G.; Loeffler, J. S.; Mc Black, P. L.; Canellos, G. P. Meta-analysis of radiation therapy with and without adjuvant chemotherapy for malignant gliomas in adults. *Cancer* **1993**, *71*, 2585–2597.
- (54) James, N. D.; Hussain, S. A.; Hall, E.; Jenkins, P.; Tremlett, J.; Rawlings, C.; Crundwell, M.; Sizer, B.; Sreenivasan, T.; Hendron, C.; Lewis, R.; Waters, R.; Huddart, R. A. Radiotherapy with or without Chemotherapy in Muscle-Invasive Bladder Cancer. *N. Engl. J. Med.* **2012**, *366*, 1477–1488.
- (55) Moore, D. H.; Ali, S.; Koh, W.-J.; Michael, H.; Barnes, M. N.; McCourt, C. K.; Homesley, H. D.; Walker, J. L. A phase II trial of radiation therapy and weekly cisplatin chemotherapy for the treatment of locally-advanced squamous cell carcinoma of the vulva: A gynecologic oncology group study. *Gynecol. Oncol.* **2012**, *124*, 529–533.
- (56) Cairncross, G.; Berkey, B.; Shaw, E.; Jenkins, R.; Scheithauer, B.; Brachman, D.; Buckner, J.; Fink, K.; Souhami, L.; Laperierre, N.; Mehta, M.; Curran, W. Phase III Trial of Chemotherapy Plus Radiotherapy Compared With Radiotherapy Alone for Pure and Mixed Anaplastic Oligodendroglioma: Intergroup Radiation Therapy Oncology Group Trial 9402. *J. Clin. Oncol.* **2006**, *24*, 2707–2714.
- (57) Peters, W. A.; Liu, P. Y.; Barrett, R. J.; Stock, R. J.; Monk, B. J.; Berek, J. S.; Souhami, L.; Grigsby, P.; Gordon, W.; Alberts, D. S. Concurrent Chemotherapy and Pelvic Radiation Therapy Compared With Pelvic Radiation Therapy Alone as Adjuvant Therapy After Radical Surgery in High-Risk Early-Stage Cancer of the Cervix. *J. Clin. Oncol.* **2000**, *18*, 1606–1613.
- (58) Miles, D.; von Minckwitz, G.; Seidman, A. D. Combination versus sequential single-agent therapy in metastatic breast cancer. *Oncologist* **2003**, *7* (Suppl 6), 13–9.
- (59) Sorenson, C. M.; Barry, M. A.; Eastman, A. Analysis of Events Associated With Cell Cycle Arrest at G₂ Phase and Cell Death Induced by Cisplatin. *Journal of the National Cancer Institute* **1990**, *82*, 749–755.
- (60) Ju, S. M.; Pae, H. O.; Kim, W. S.; Kang, D. G.; Lee, H. S.; Jeon, B. H. Role of reactive oxygen species in p53 activation during cisplatin-induced apoptosis of rat mesangial cells. *European review for medical and pharmacological sciences* **2014**, *18*, 1135–41.